PAPER Special Section on Position Papers Exploring Innovative Intelligence and Technologies in Communications

Concept of Chaos-Based Hierarchical Network Control and Its Application to Transmission Rate Control

Masaki AIDA[†a)], ***Member***

SUMMARY Information networks are an important infrastructure and their resources are shared by many users. In order to utilize their resources efficiently, they should be controlled to prevent synchronization of user traffic. In addition, fairness among users must be assured. This paper discusses the framework of transmission rate control based on chaos. There are two different characteristics that coexist in chaos. One is that the state in the future is extremely sensitive to the initial condition. This makes it impossible to predict the future state at a fine level of detail. The other is the structural stability of macroscopic dynamics. Even if the state is uncertain on the microscopic scale, state dynamics on the macroscopic scale are stable. This paper proposes a novel framework of distributed hierarchical control of transmission rate by interpreting the coexistence of chaos as microscopic fairness of users and macroscopic stable utilization of networks.

key words: *chaos, distributed control, hierarchy, flow control*

1. Introduction

This paper discusses a novel framework of autonomous distributed network control that is based on chaos. Autonomous distributed control in networks is required to utilize the relationship between microscopic rules of local actions and the macroscopic states generated by the collective results of local actions. Therefore, the framework of autonomous distributed control suggests the existence of a hierarchical structure with respect to the dimensions of space/time scales. The key idea of this paper lies in its proposal of a correspondence between the network dynamics of different scales and the micro- and macroscopic characteristics of chaos.

1.1 Distributed Network Control and Hierarchy with Respect to the Dimensions of Space/Time Scales

Since current information networks are large-scale and high-speed systems, the only scalable control approach is autonomous distributed control. This is because centralized control demands detailed information of current system state of all system components, while autonomous distributed control needs only local information of component state.

Autonomous distributed control requires to utilize the relationship between the microscopic rules of autonomous control actions based on local information, and macroscopic global states which is generated from the collective results of the autonomous actions of local control. In other words, effective system control demands an understanding of the relationship between micro- and macroscopic states, that is, different hierarchies, with respect to the dimensions of space/time scales.

Research on a framework of autonomous distributed control includes a scheme based on a partial differential equation [1]. For this scheme, we introduce a framework that the temporal evolution of a system expressed by partial differential equations; it can be interpreted that it describes local action rules that are equivalent to autonomous distributed control. Next, we interpret the solution of the partial differential equation as the global state of the network; that is, the macroscopic state is generated from the collective effects of microscopic local actions of the corresponding autonomous distributed control. By applying this framework, we can obtain the desired global state of the entire network even though each network element acts autonomously based on its local information. The desired global state can includes properties such as load balancing, congestion avoidance, and clustering.

In this paper, by utilizing the characteristics of chaos, we introduce a novel framework of autonomous distributed control that can simultaneously meet requirements placed on both micro- and macroscopic states on different hierarchies. The characteristics of chaos and a way of applying them to hierarchical network control are described in the next subsection.

1.2 Concept of Chaos-Based Hierarchical Network Control

In order to utilize network resources effectively, stochastic model-based control schemes using random numbers have been well studied. As an example, let us consider transmission rate control (or flow control).

The well-known TCP global synchronization problem [2] is as follows. Let us consider the situation that there are some flows that have the same round-trip time (RTT) and they lose packets simultaneously due to congestion. Then the control response of setting window size (increase and decrease) for their flows are synchronized yielding temporal concentration of traffic. This phenomenon degrades network efficiency.

Random Early Detection (RED) is one approach introduced to tackle TCP global synchronization [2]. In order to

Manuscript received March 13, 2014.
Manuscript revised July 25, 2014.

[†]The author is with the Graduate School of System Design, Tokyo Metropolitan University, Hino-shi, 191-0065 Japan.
a) E-mail: aida@tmu.ac.jp

DOI: 10.1587/transcom.E98.B.135

prevent synchronization, it is necessary to avoid the simultaneous loss of packets belonging to many flows. RED tries to avoid congestion by dropping packets randomly before the router buffer becomes full. Since heavy flows are the most frequent cause of congestion, shrinking the window size of these flows is an effective way of avoiding congestion. Consequently, RED realizes congestion avoidance by dropping arriving packets randomly when buffer utilization is high. It is obvious that heavy flows will experience packet dropping more frequency than other flows. However, because it is stochastic-based action, low-rate flows may suffer packet dropping, particular when there are many low-rate flows. For example, let us consider the situation that there are 100 low-rate (equal) flows, and only one high-rate flow (100 times the low rate). If we drop an incoming packet randomly, the probability that the dropped packet is from a low-rate flow is $1/2$. If low-rate flow packets are dropped, congestion avoidance becomes ineffective and flow fairness is worsened.

This paper introduces a novel framework of chaos-based hierarchical network control. The objective of chaos-based hierarchical control is to keep fairness among flows by regulating the flow of the highest rate in a deterministic manner, and simultaneously to utilize network resources effectively by preventing traffic concentrations.

Chaos appears in certain deterministic models. Here, a Lorenz model (a typical example of chaos) is a dynamic model represented by the following equations [3]:

$$\frac{\mathrm{d}x}{\mathrm{d}t} = -px + py, \quad \frac{\mathrm{d}y}{\mathrm{d}t} = -xz + qx - y, \quad \frac{\mathrm{d}z}{\mathrm{d}t} = xy - sz,$$

where x, y, z are variables and p, q, s are constants. Figure 1 shows two trajectories (red and blue) of (x, y, z) when we set $p = 10$, $q = 28$, $s = 8/3$ [3]. The most well-known characteristic of chaos is that the future is extremely sensitive to the initial condition. By tracking a trajectory (in microscopic scale) in its state space, we can know what its state in the future will be, completely, at least in principle. However, since any minute fractional change in the initial conditions leads rapidly to a massive divergence in the trajectory, in practice we unable to predict the state. In this sense, the trajectory in the state space observed by tracking the trajectory on a microscopic scale is unstable, and looks random to us. On the other hand, we can recognize that the trajectory forms the same stable attractor (Lorenz attractor) on a macroscopic scale, see Fig. 1.

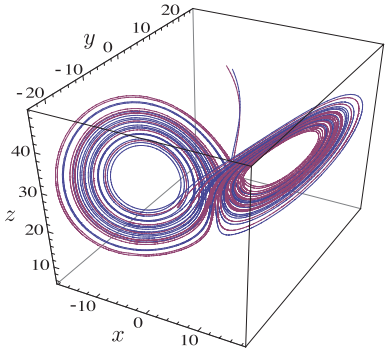

Fig. 1 Typical example of chaos: Lorenz attractor.

In this paper, we use the above two characteristics of chaos to create micro- and macroscopic performance measures of networks, respectively, and propose a novel framework of distributed hierarchical control of transmission rate. The features of the proposed control framework are summarized as follows.

- We regulate only the flow with maximum transmission rate, if needed, by a deterministic action rule, in order to keep fairness among users. Simultaneously, due to the effect of chaos, transmission rates of flows look random. This prevents synchronization of flow transmission rates and avoids temporal concentration of traffic, while keeping fairness among users.
- As the shape of strange attractor is stable on the macroscopic scale, we can have stable global performance (throughput) of the networks. Simultaneously, global performance is controllable through local action rules applied by autonomous distributed control on the microscopic scale.

Since this proposed framework is not restricted to any specific model of chaos, it is expected to support various models of chaos.

2. Chaos Generated from Coupled Oscillators and Transmission Rate Control

This section details a concrete distributed algorithm of transmission rate control based on chaos generated from coupled oscillators. Figure 2 shows our network model of transmission rate control. There are n senders that are accommodated in a router and each sender sends a traffic flow. Transmission rate control can be implemented in various ways, for example, window control like TCP or explicit specification of the allowable rate from the networks to the sender. For flexibility, this paper makes no assumption as to the explicit flow rate control adopted.

2.1 Preliminary: Basic Rule of Coupled Ocsillators

We assume that the transmission rate of each flow is determined by coupled oscillators. This section introduces the coupled relaxation oscillators used in this paper, and investigates the chaos generated from the oscillators.

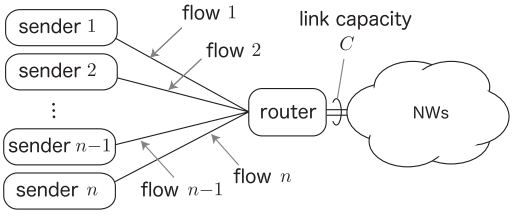

Fig. 2 Network model of transmission rate control.

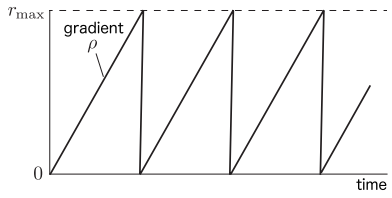

Fig. 3 Relaxation oscillator between $[0,\ r_{\max}]$.

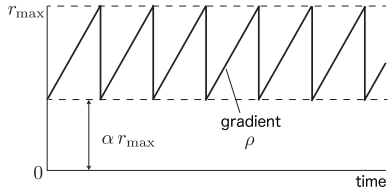

Fig. 4 Relaxation oscillator between $[\alpha r_{\max},\ r_{\max}]$ $(\alpha < 1)$.

There are two types of oscillatory phenomena, one is free oscillation and the other is coupled oscillation. Free oscillation has a specific frequency. Examples of free oscillation, the temporal evolution of the displacement $r(t)$ of relaxation oscillators, are shown in Figs. 3 and 4. The displacement $r(t)$ of the oscillator increases with the rate of increase ρ; if the displacement reaches a threshold $r_{\max}$, the displacement relaxes to 0 or to $\alpha\, r_{\max}$, where $0 \le \alpha < 1$. The corresponding temporal evolution equations are

$$\frac{\mathrm{d}r(t)}{\mathrm{d}t} = \rho - \rho\, r_{\max}\, \delta(r(t) - r_{\max}), \tag{1}$$

$$\frac{\mathrm{d}r(t)}{\mathrm{d}t} = \rho - \rho\,(1-\alpha)\, r_{\max}\, \delta(r(t) - r_{\max}), \tag{2}$$

where $\delta(\cdot)$ is Dirac's delta function. The role of the delta function in these temporal evolution equations is explained in Appendix A. These relaxation oscillators are of interest since their operation looks like the window control of TCP Reno [4].

On the other hand, coupled oscillators are a system consisting of two or more oscillators that mutually influence each other. Unlike free oscillations, coupled oscillators do not necessarily have a specific frequency, and they often exhibit complex behaviors. Let us consider the model of coupled relaxation oscillators known as Ito's great earthquake model [5], [6].

There are n oscillators (n is the number of flows) and let the displacement of oscillator i ($i = 1, \ldots, n$) at time t be $r_i(t)$. In addition, each oscillator i has an adjacent relation with oscillators $i+1$ and $i-1$, and the periodic boundary conditions $r_0(t) := r_n(t)$, $r_{n+1}(t) := r_0(t)$ are assumed. There are many concrete ways to assign adjacent relation to flows, for example, ascending order of the flow setup time, or the ascending order of terminal IDs. The rule of the coupled oscillator model is described as follows.

- The displacement $r_i(t)$ for each oscillator i increases at the rate of increase of ρ or $\beta\rho$ (here, β and ρ are constants, and $0 \le \beta < 1$, $\rho > 0$).

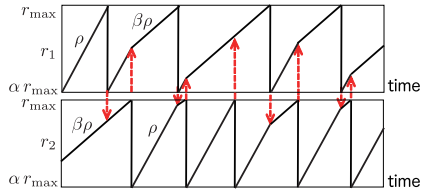

Fig. 5 Example of temporal evolution of displacements of coupled oscillators for $n = 2$.

- When displacement $r_j(t)$ for oscillator j reaches threshold $r_{\max}$, then
  - for oscillator j, displacement $r_j(t)$ is relaxed to $\alpha\, r_{\max}$ (here, α is a constant and $0 \le \alpha < 1$) and the rate of increase of $r_j(t)$ is reset to ρ, and
  - for the adjacent oscillators of oscillator j, the increase rate of the transmission rates $r_{j-1}(t)$ and $r_{j+1}(t)$ for oscillators $j-1$ and $j+1$ are reset to $\beta\rho$. If the increase rate is $\beta\rho$ already, it is kept as is.

Ito's great earthquake model is the case of $\alpha = 0$. A simple example of the temporal evolution of displacements for $n = 2$ is given by Fig. 5.

Let the set of oscillators adjacent to oscillator i be $N(i)$. The temporal evolution of the displacements of the coupled oscillators can be described by the following equations.

$$\frac{\mathrm{d}r_i(t)}{\mathrm{d}t} = s_i(t) - s_i(t)\,(1-\alpha)\, r_{\max}\, \delta(r_i(t) - r_{\max}), \tag{3}$$

where the temporal evolution of the rate of increase $s_i(t)$ is expressed as

$$\frac{\mathrm{d}s_i(t)}{\mathrm{d}t} = \sum_{j \in N(i)} s_j(t)\, \Big(\beta\rho - s_j(t)\Big)\, \delta(r_j(t) - r_{\max}) + s_i(t)\, (\rho - s_i(t))\, \delta(r_i(t) - r_{\max}). \tag{4}$$

Note that the temporal evolution of oscillator i can be determined only by the displacements of oscillator i itself and its adjacent oscillators. Information about all oscillators is not necessary. This means this system of coupled relaxation oscillators (or the corresponding transmission rate control) can be implemented by local autonomous actions.

2.2 Chaos Generated by Coupled Oscillators

This subsection examines the chaos generated by the above coupled relaxation oscillators by following the discussion in [5], [6]. In addition, we discuss technical issues in applying the coupled relaxation oscillator model to transmission rate control.

Let us consider the coupled oscillator system for $n = 2$. The temporal evolution of the two oscillators can be represented as a trajectory in the state space $[\alpha r_{\max},\ r_{\max}] \times [\alpha r_{\max},\ r_{\max}]$, that has periodic toroidal boundaries, as shown in Fig. 6. Here, the horizontal and vertical axes of Fig. 6 denote $r_1(t)$ and $r_2(t)$, respectively. The trajectory proceeds to the upper right with time at the gradient of $1/\beta$ or

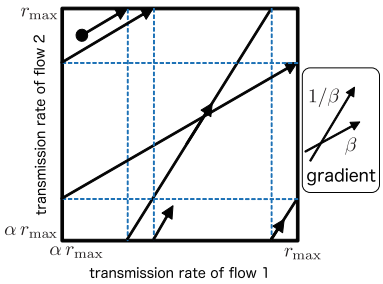

Fig. 6 Trajectory in the state space of a coupled oscillator system.

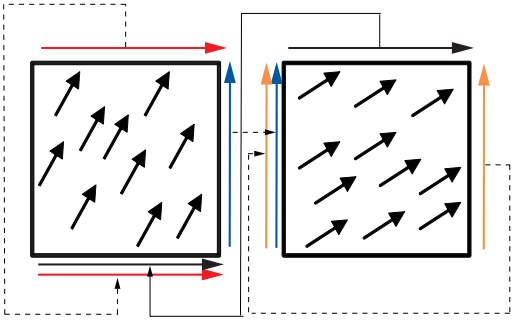

Fig. 7 State space described by two vector fields.

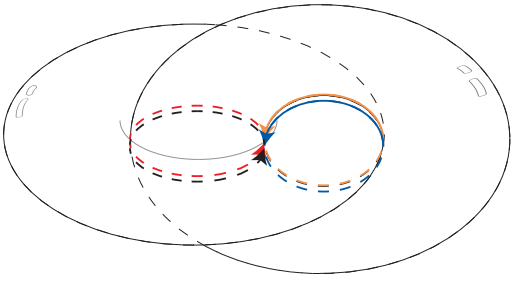

Fig. 8 Topology of the glued state space.

β. This is because if the rate of increase of one oscillator is ρ, the rate of the other oscillator is $\beta\rho$. In addition, both rates are altered only when the displacement of the oscillator having the rate of $\beta\rho$ reaches $r_{\max}$. This state space is a divalent vector field, that is, there are two possibilities in the gradient of the trajectory even if the current position on the state space is given. This means the trajectory depends on the past state.

We introduce a representation of the equivalent state space based on a monovalent vector field. In this representation, the trajectory is completely determined if the current position on the state space is given. Let us consider two vector fields with gradient $1/\beta$ and β, as shown in Fig. 7. Next, we glue the corresponding colored edges of the two vector fields together, so that the arrows match, as shown in Fig. 7. The topology of the state space obtained from gluing the two vector fields is shown in Fig. 8. It is known that the structure shown in Figs. 7 and 8 is topologically equivalent to the Lorenz attractor shown in Fig. 1 [5], [6].

Next, we introduce a recursive rule that describes a

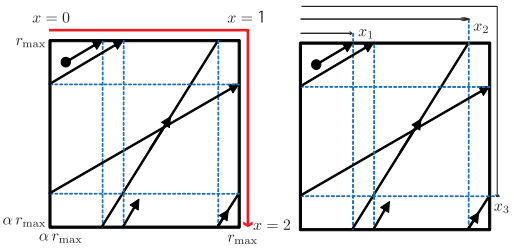

Fig. 9 Parameterization of the position at the time of relaxation.

state transition between a sequence of time points of displacement relaxations of the oscillators. First, we define a representation of the state at the time that one of the oscillators reaches threshold $r_{\max}$, as follows. When the oscillator reach the threshold, the trajectory reaches the upper-boundary or the right-boundary, we measure the position by $x \in [0, 2]$ along these boundary edges as shown as red line in Fig. 9. If the trajectories intersect the upper-boundary, we denote the position by parameter x ($0 \le x \le 1$), which corresponds to the values of $r_1(t)$ and $r_2(t)$ given by

$$(r_1(t),\ r_2(t)) = ((\alpha + (1-\alpha)\,x)\,r_{\max},\ r_{\max}),$$

and if the trajectories intersect the right-boundary, we denote the position by parameter x ($1 \le x \le 2$), which corresponds to the values of $r_1(t)$ and $r_2(t)$ given by

$$(r_1(t),\ r_2(t)) = (r_{\max},\ (1-(1-\alpha)\,(x-1))\,r_{\max}).$$

Let $x_m \in [0, 2]$ be the state at the m-th time ($m = 1, 2, \ldots$). Let the recursive relation between x_m and x_{m+1} be f, that is,

$$x_{m+1} = f(x_m). \tag{5}$$

Then, f is expressed as

$$f(x) = \begin{cases} x+\beta, & (0 \le x < 1-\beta), \\ \dfrac{1}{\beta}\,x + 2 - \dfrac{1}{\beta}, & (1-\beta \le x < 1), \\ \dfrac{1}{\beta}\,x - \dfrac{1}{\beta}, & (1 \le x < 1+\beta), \\ x-\beta, & (1+\beta \le x < 2). \end{cases} \tag{6}$$

It can be illustrated as in Fig. 10. Note that the gradient of that line exceeds 1 in the period of $x \in [1-\beta,\ 1+\beta]$ if $\beta < 1$. This fact is why chaos is generated. The offset of red and blue lines expands geometrically with each reflection at $f(x)$ in the period because the gradient $1/\beta > 1$. A minute fractional difference between two trajectories diverges geometrically. As shown by the above, chaos can be generated from a very simple deterministic operation.

The above result can be extended to the case for n oscillators (n flows). If there is any effect from other oscillators on these two oscillators, it is the effect that the ratio of increase changes from ρ to $\beta\rho$. From the rule of the coupled oscillators, the case where two adjacent oscillators simultaneously have the rate of increase of ρ never occurs. Accordingly, the other oscillators have an effect only when the

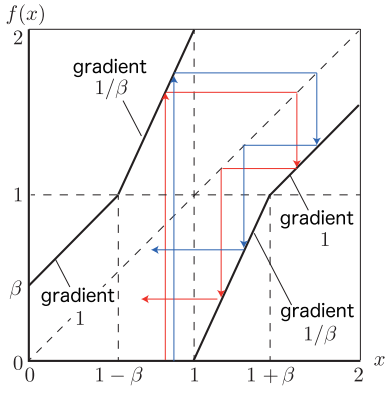

Fig. 10 Recursive relation of the state at the relaxation time.

rates of increase of both oscillators coincide at $\beta\rho$. This effect merely keeps the relationship between two oscillators for a while until the next relaxation time, and it does not alter the mechanism of chaos generation.

Since the above coupled-oscillator system generates chaos, the trajectory in the state space is extremely sensitive to the initial condition; any slight difference from the state of the present time yields wildly divergent results in the future, and we cannot predict the state in the future. By determining the transmission rate as displacement $r_i(t)$, transmission rates for flows appear to be randomized. This ensures that we can avoid the temporal concentration of traffic. In addition, since the relaxation of the transmission rate occurs only for the flow that has the maximum transmission rate by the deterministic rule, we can expect that the fairness among flows is kept. These effects are microscopic aspects of hierarchical control. Moreover, we expect that we can control the throughput while keeping these randomized and fair state on the microscopic flow level. By tuning the values of parameters α, β and $r_{\max}$, deformation of the macroscopic form of the strange attractor occurs, which results in a change in throughput. This effect is a macroscopic aspect of hierarchical control.

On the other hand, since the threshold $r_{\max}$ of the coupled oscillators is set to individual flows, the relaxation may occur even if the network is not congested. In addition, the relationship between $r_{\max}$ and the capacity of network resource is unclear. Thus, the transmission rate control is necessary to be improved by considering the capacity of network resource.

3. Transmission Rate Control Considering Restriction of the Capacity of Link Bandwidth

In the above mentioned transmission rate control, relaxation of transmission rate occurs when the rate reaches its threshold even if the capacity of network resource left. In actual network, relaxation of transmission rate should occur only when the sum of transmission rate for all flows reaches the capacity of the accommodated link. This section investigates such modification of transmission rate control and clarifies the characteristics of the modified control. As results, the modified control, unfortunately, is not an autonomous distributed control and chaos does not appear. Finally, this section discusses an approach to restore the framework of chaos-based autonomous distributed control.

3.1 Modified Transmission Rate Control

The rule of the modified coupled oscillator model is described as follows.

- The displacement $r_i(t)$ for oscillator i increases at the rate of increase of ρ or $\beta\rho$ (here, β and ρ are constants, and $0 \le \beta < 1, \rho > 0$).
- When the sum of displacements $\sum_i r_i(t)$ reaches the capacity of link C, we choose the flow j that has the maximum transmission rate and
  - for the oscillator j, the displacement $r_j(t)$ is relaxed to $\alpha\, r_j(t)$ (here, α is a constant and $0 \le \alpha < 1$) and the rate of increase of $r_j(t)$ is reset to ρ, and
  - for adjacent oscillators of oscillator j, the increase rate of the transmission rates $r_{j-1}(t)$ and $r_{j+1}(t)$ for oscillators $j-1$ and $j+1$ are reset to $\beta\rho$. If the increase rate is $\beta\rho$ already, it is kept as is.

Note that this model requires not only transmission rates for adjacent flows but also the sum of transmission rates for all flows. This means that the modified control does not work as in autonomous distributed manner.

Let the set of oscillators adjacent to oscillator i be $N(i)$, and $k(t) := \arg\max_j r_j(t)$. The temporal evolution of the displacements of the modified coupled oscillators can be described by the following equations,

$$\frac{\mathrm{d}r_i(t)}{\mathrm{d}t} = s_i(t) - (1-\alpha)\, r_i(t)\, \delta_{i,k(t)}\, \delta\left(\sum_j r_j(t) - C\right) \sum_j s_j(t), \tag{7}$$

where the temporal evolution of the rate of increase $s_i(t)$ is expressed as

$$\frac{\mathrm{d}s_i(t)}{\mathrm{d}t} = \sum_{\ell \in N(i)} (\beta\rho - s_i(t))\, \delta_{\ell,k(t)}\, \delta\left(\sum_j r_j(t) - C\right) \sum_j s_j(t) + (\rho - s_i(t))\, \delta_{i,k(t)}\, \delta\left(\sum_j r_j(t) - C\right) \sum_j s_j(t). \tag{8}$$

For simplicity, let us consider the case of $n = 2$ and examine its state space. Since the sum of transmission rates is restricted as $r_1(t) + r_2(t) \le C$, the state space can be illustrated as Figs. 11 and 12. Figure 11 is a special case of Fig. 12 with $\alpha = 0$.

Next, we consider the recursive rule that describes a state transition between the time points of the relaxation of the transmission rate. First, we define a representation of the state at the time that the sum of transmission rate reaches C, as follows. When the sum of transmission rates reaches

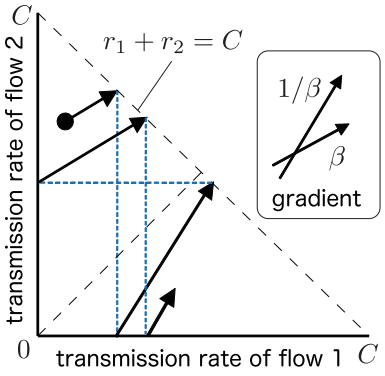

Fig. 11 Trajectory in the state space of the modified coupled oscillator for $\alpha = 0$.

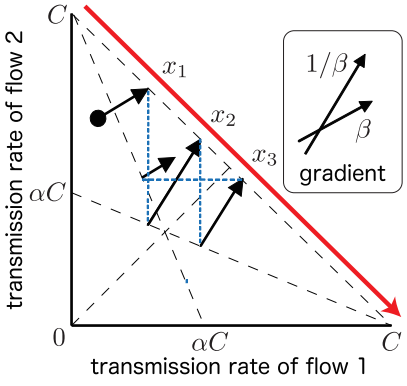

Fig. 12 Trajectory in the state space of the modified coupled oscillator and parameterization of the position at the time of relaxation.

C, the trajectory reaches the line of $r_1(t) + r_2(t) = C$. We parameterize that point by $x \in [0, 1]$ along the red line shown in Fig. 12. The parameter x corresponds to the position $(r_1(t), r_2(t)) = (xC, (1-x)C)$.

Let $x_m \in [0, 1]$ be the state at the m-th time ($m = 1, 2, \ldots$). Let the recursive relation between x_m and x_{m+1} be g, that is,

$$x_{m+1} = g(x_m). \tag{9}$$

Then, g is expressed as

$$g(x) = \begin{cases} \dfrac{1+\alpha\beta}{1+\beta}\, x + \dfrac{\beta(1-\alpha)}{1+\beta}, & (0 \le x < 1/2), \\ \dfrac{1+\alpha\beta}{1+\beta}\, x, & (1/2 \le x \le 1). \end{cases} \tag{10}$$

Figure 13 illustrates $g(x)$. The red line show an example of the sequence of x_m and it approaches the attractor shown by the blue square. The x-coordinates of the vertices of the square as the attractor are

$$x_- = \frac{1+\alpha\beta}{2+\beta+\alpha\beta}, \quad x_+ = \frac{1+\beta}{2+\beta+\alpha\beta}. \tag{11}$$

Since all trajectories are subsumed by this attractor, chaos does not appear in this control. Let us investigate the behavior around the attractor. For displacement ϵ from attractor

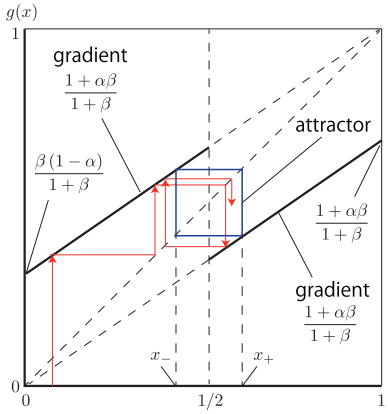

Fig. 13 Recursive relation of the state at the relaxation time and the attractor.

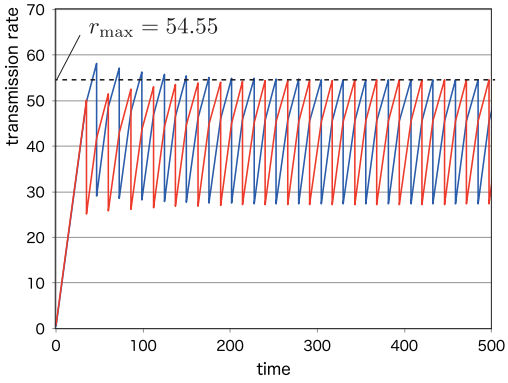

Fig. 14 Temporal evolution of transmission rates for the improved control ($n = 2$).

x_-, ie. for $x = x_- + \epsilon$, we have

$$\begin{aligned} g(x_- + \epsilon) &= \frac{1+\alpha\beta}{1+\beta}\left(\frac{1+\alpha\beta}{2+\beta+\alpha\beta} + \epsilon\right) + \frac{\beta(1-\alpha)}{1+\beta} \\ &= \frac{1+\beta}{2+\beta+\alpha\beta} + \frac{1+\alpha\beta}{1+\beta}\,\epsilon, \\ \{g \circ g\}(x_- + \epsilon) &= \frac{1+\alpha\beta}{1+\beta}\,\frac{1+\beta}{2+\beta+\alpha\beta} + \left(\frac{1+\alpha\beta}{1+\beta}\right)^2 \epsilon \\ &= x_- + \left(\frac{1+\alpha\beta}{1+\beta}\right)^2 \epsilon. \end{aligned} \tag{12}$$

Therefore, the displacement from the attractor geometrically decreases if $\alpha < 1$. Note that the attractor exists not only for $\beta < 1$, but also for $\beta \ge 1$. In addition, unlike coupled oscillators having individual thresholds, shown in the previous section, chaos does not appear in either $\beta < 1$ or $\beta \ge 1$ cases.

3.2 The Behavior of the Transmission Rate Maximum

This subsection investigates the actual temporal evolution of transmission rate for the modified control. Figure 14 shows a typical example of the temporal evolution of transmission rate of each flow, from a certain initial condition. The number of flows is $n = 2$, and $\alpha = 1/2$, $\beta = 1/2$ and link ca-

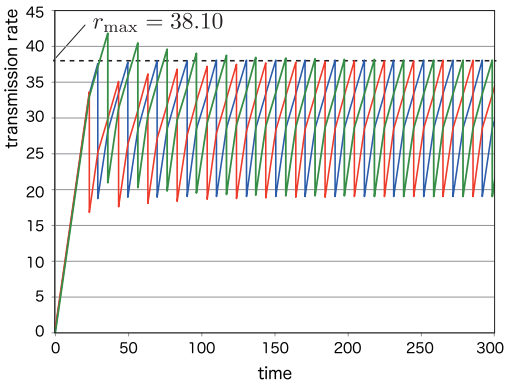

Fig. 15 Temporal evolution of transmission rates for the improved control ($n = 3$).

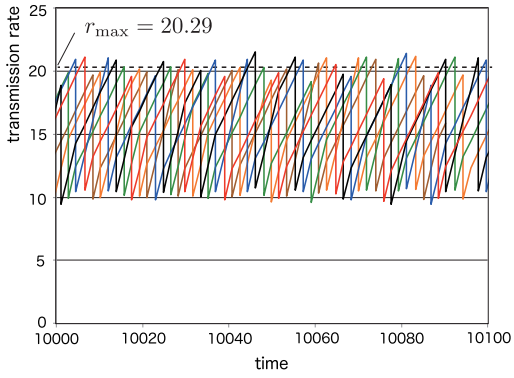

Fig. 16 Temporal evolution of transmission rates for the improved control ($n = 6$).

pacity is $C = 100$. Attractors x_+ and x_- shown in Fig. 13 correspond to the phenomenon that the transmission rates of the two flows are synchronized but with opposite phase. Although chaos does not appear, it is not a problem. Synchronization in opposite phase is ideal for utilizing network resources efficiently.

Figure 15 shows a similar evaluation for $n = 3$. Even in this case, transmission rates of the three flows synchronize, and their phases are equally offset. Although chaos does not appear, this is also an ideal state for utilizing network resources efficiently.

In the case of synchronization with equi-offset phases, we can obtain the maximum value of transmission rate, $r_{\max}$, and the period of the cycle of transmission rate, T, as follows:

$$r_{\max} = \frac{2\,(1 + (n-1)\,\beta)}{n\,(2 + (n-1)\,\beta + (n-1)\,\alpha\beta)}\,C, \tag{13}$$

$$T = \frac{2\,(1-\alpha)}{\rho\,(2 + (n-1)\,\beta + (n-1)\,\alpha\beta)}\,C. \tag{14}$$

The derivations of (13) and (14) are shown in Appendix B. The values of $r_{\max}$ obtained from (13) are shown in Figs. 14 and 15. We can recognize that the transmission rates are quickly synchronized.

For $n = 2$ and 3, the set of a certain flow and its adjacent flows contains all flows. This is why all the flows can be synchronized by mere local interaction between adjacent flows. However, flows do not synchronize for large n as shown by the following example. Figure 16 shows a similar evaluation for $n = 6$. Even though sufficient time has elapsed, the transmission rates exhibit complex patterns and remain unsynchronized. However, since we do not understand regularity in the general case, we cannot affirm that the temporal concentration of traffic would never occur.

From the above consideration, the modified control does not generate chaos in general. Thus, the modified control does not follow the framework of chaos-based hierarchical control shown in Sect. 1.2. Even if chaos does not appear, network resource can be effectively utilized if the transmission rates are synchronized with equi-offset phases. However, in general, such synchronization does not occur.

Table 1 Comparison of experimental and estimated values of $r_{\max}$.

n	5	10	50	100	500	1000
experiments	23.99	12.57	2.57	1.29	.258	.129
estimation	24.00	12.57	2.63	1.32	.266	.133

In addition, since the modified control requires information of all flows, it cannot be implemented as autonomous distributed control.

3.3 Towards Restoration of Chaos-Based Hierarchical Control Mechanism

The technical issues posed by transmission rate control shown in Sect. 2 are rooted in the issue of finding some way of determining oscillator thresholds, $r_{\max}$, from network resources. As shown in Sect. 3.2, if the transmission rates for flows are synchronized with equi-offset phases, we can calculate the threshold by (13). Since this is the value in the ideal case, let us consider the meaning of (13) for large n.

Figure 16 shows the values of $r_{\max}$ obtained from (13). We can recognize that the values at which the relaxation occurs are not the same but they are distributed closely around $r_{\max}$. Table 1 shows a comparison between the experimental and estimated values for various n, where $\alpha = 1/2, \beta = 1/2$ and $C = 100$. The experimental values are the averages of the values at which relaxation occurs, and the estimated values are obtained from (13). We can recognize that (13) closely follows the experimental value.

Consequently, we might be able to use the value of $r_{\max}$ obtained from (13) as the threshold $r_{\max}$ of the chaos-based transmission rate control described in Sect. 2. This means that by applying threshold (13), chaos-based transmission rate control can efficiently utilize the capacity, C, link bandwidth. In addition, since it is guaranteed to generate chaos, we can expect that it is a hierarchical control mechanism offering both fairness in the microscopic individual flows and efficient utilization of macroscopic system resources. Note that the number of flows used in (13), n, is not a local information of flow. Thus the real-time updated value of n cannot be used in the framework of autonomous distributed control. However, since the value of n may not need to be updated

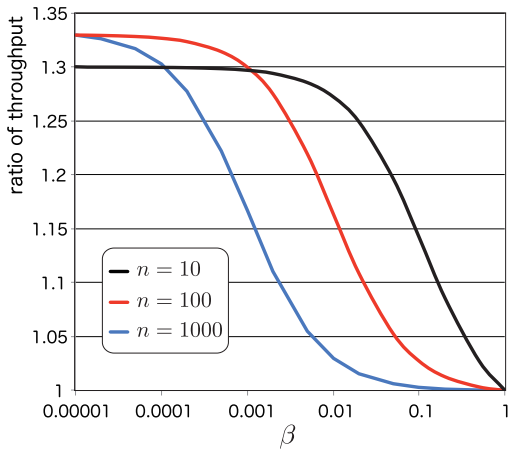

Fig. 17 Ratio of Throughput with Respect to β.

frequently, unlike the transmission rates of flows, we expect that chaos-based transmission rate control can implemented as an autonomous distributed manner.

In the case that the transmission rates for flows synchronize with equi-offset phases (i.e., the ideal case), the average throughput per flow. $\langle r \rangle$ is obtained as

$$\langle r \rangle = \alpha\, r_{\max} + \frac{(1-\alpha)\,(2n-1+(n-1)^2\,\beta)}{2n\,(1+(n-1)\,\beta)}\, r_{\max}. \quad (15)$$

The derivation of (15) is shown in Appendix B. On the other hand, for non-coupled relaxation oscillators ($\beta = 1$) between the period $[\alpha r_{\max},\, r_{\max}]$, the average throughput per flow is $(1+\alpha)\, r_{\max}/2$. In general, $\langle r \rangle$ is greater than $(1+\alpha)\, r_{\max}/2$ for $\beta < 1$. Figure 17 plots their ratio for $\alpha = 1/2$, $C = 100$, and $n = 10, 100, 1000$. By tuning the value of β, the average throughput improves by about 30%. Since this characteristic is due to the form of the strange attractor of the chaos-based control, we expect that chaos-based hierarchical control can improve the throughput.

4. Conclusion

This paper has introduced a novel framework of hierarchical network control. This framework is based on two characteristics of chaos: the unpredictability of the microscopic state in the future, and the macroscopic stability of the global dynamics. The two characteristics are interpreted as fairness among users and network performance, respectively. By applying the framework to transmission rate control, this paper also described an approach to realizing a distributed algorithm of chaos-based hierarchical control.

Acknowledgment

The author would like to thank Prof. Masayuki Murata of Osaka University and Prof. Jean Walrand of UC Berkeley for their helpful comments. The author also thanks Mr. Liu Yongchao of Tokyo Metropolitan University for his help with numerical experiments. This research is supported by a Grant-in-Aid for Challenging Exploratory Research No. 25540032 (2013–2015) from the Japan Society for the Promotion of Science.

References

[1] M. Aida, "Using a renormalization group to create ideal hierarchical network architecture with time scale dependency," IEICE Trans. Commun., vol.E95-B, no.5, pp.1488–1500, May 2012.
[2] S. Floyd and V. Jacobson, "Random early detection gateways for congestion avoidance," IEEE/ACM Trans. Netw., vol.1, no.4, pp.397–413, Aug. 1993.
[3] E.N. Lorenz, "Deterministic nonperiodic flow," J. Atmospheric Science, vol.20, pp.130–141, 1963.
[4] M. Allman, V. Paxson, and W. Stevens, "TCP congestion control (RFC 2581)," http://www.ietf.org/rfc/rfc2581.txt
[5] Y. Oono, Introduction to Nonlinear World, University of Tokyo Press, 2009. (in Japanese)
[6] K. Ito, Y. Oono, H. Yamazaki, and K. Hirakawa, "Chaotic behavior in great earthquakes coupled relaxation oscillator model, billiard model and electronic circuit model," J. Physical Society of Japan, vol.49, no.1, pp.43–52, 1980.
[7] Y. Takahashi, C. Takano, Y. Sakumoto, M. Aida, "Transmission rate control utilizing chaotic nature of coupled oscillators," Intelligent Networking and Collaborative Systems (INCoS2012), pp.126–131, Bucharest, Romania, Sept. 2012.

Appendix A: The Role of Dirac's Delta Function in (2)

In order to understand the role of the delta function in the right-hand side of the temporal evolution equation (2) of the relaxation oscillator, let us consider, as the first step, only the first term on the right-hand side in (2). That is,

$$\frac{\mathrm{d}r(t)}{\mathrm{d}t} = \rho.$$

By integrating with respect to t, we obtain

$$r(t) = \rho\, t + r(0).$$

This function yields the increasing line with gradient of ρ shown in Fig. 4. Before considering the role of the delta function in the next step, let us recall the characteristics of the delta function. That is,

$$\delta(x) = \begin{cases} \infty, & (x = 0), \\ 0, & (\text{otherwise}), \end{cases}$$

and

$$\int_{-\infty}^{\infty} \delta(x)\, \mathrm{d}x = 1.$$

If $r(0) = 0$ and the displacement reaches the threshold for the first time at time s,

$$r(s) = \rho\, s = r_{\max}.$$

By integrating both sides of (2), we have

$$r(s) = \int_0^s \frac{\mathrm{d}r(t)}{\mathrm{d}t}\, \mathrm{d}t$$

$$
\begin{aligned}
&= \rho\, s - \rho\,(1-\alpha)\, r_{\max} \int_0^s \delta(r(t) - r_{\max})\, \mathrm{d}t \\
&= r_{\max} - (1-\alpha)\, r_{\max} \int_0^s \delta(r(t) - r_{\max})\, \rho\, \mathrm{d}t \\
&= r_{\max} - (1-\alpha)\, r_{\max} \int_0^s \delta(r(t) - r_{\max})\, \frac{\mathrm{d}r(t)}{\mathrm{d}t}\, \mathrm{d}t \\
&= r_{\max} - (1-\alpha)\, r_{\max} \int_{t=0}^s \delta(r(t) - r_{\max})\, \mathrm{d}r(t) \\
&= r_{\max} - (1-\alpha)\, r_{\max} \\
&= \alpha\, r_{\max}.
\end{aligned}
$$

This result means that the displacement relaxes to the value of $\alpha\, r_{\max}$ when the displacement reaches threshold $r_{\max}$. Even after relaxation occurs, relaxation will occur whenever the displacement reaches the threshold. As for (3), it is a special case of (4) with $\alpha = 0$.

Even for other temporal evaluation equations including the delta function, the delta function plays the same role with regard to relaxation.

Appendix B: The Derivations of (13) and (14)

Let us consider the situation that the transmission rates for n flows are synchronized with equi-offset phases. The range of oscillation of the transmission rate is $[\alpha\, r_{\max},\, r_{\max}]$. Figure A·1 shows this situation for $n = 6$ and the thick line tracks the transmission rate of a certain flow. Each flow has two phases: one is the period with the rate of increase in the transmission rate is ρ, and the other is the period with $\beta\rho$. If the length of the first period is x, the period of the cycling of the transmission rate, T, is $T = n\, x$. After relaxation of the transmission rate, the rate of increase in the transmission rate is ρ in the first period of length x, and after that the rate of increase is $\beta\rho$. When the transmission rate reaches the threshold $r_{\max}$, the sum of transmission rates for all flow reaches the capacity of link C, and, simultaneously, the largest transmission rate, $r_{\max}$, is relaxed to $\alpha\, r_{\max}$. At the time immediately before a relaxation occurs, the sum of the transmission rates is C, and we have

$$
\begin{aligned}
&n\,(\alpha\, r_{\max} + \rho\, x) + \beta\rho\,(x + 2x + \cdots + (n-1)\, x) \\
&\quad = n\,(\alpha\, r_{\max} + \rho\, x) + \beta\rho\, x\, \frac{n\,(n-1)}{2} \\
&\quad = C. \qquad \text{(A·1)}
\end{aligned}
$$

Here, since the period of cycle of transmission rate is $T = n\, x$,

$$
\alpha\, r_{\max} + \rho\, x + \beta\rho\, x(n-1) = r_{\max},
$$

and we have

$$
x = \frac{(1-\alpha)\, r_{\max}}{\rho\,(1 + \beta\,(n-1))}. \qquad \text{(A·2)}
$$

By substituting (A·2) into (A·1), we obtain (13) and (14).

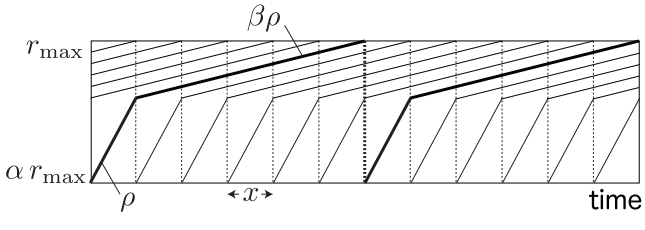

Fig. A·1 Threshold $r_{\max}$ under the situation that n flows are synchronized with equi-offset phases.

Appendix C: The Derivation of (15)

To calculate the throughput of each flow under the situation that n flows are synchronized with equi-offset phases, we calculate the average transmission rate for one period of the cycle. Figure A·2 shows the transmission rate during one cycle where $h := \rho x$. To calculate the area of the transmission rate during one cycle, we divide it into four parts (A), (B), (C) and (D), as shown in Fig. A·2. From (A·2) and $h = \rho x$, we have

$$
h = \frac{1-\alpha}{1 + \beta\,(n-1)}\, r_{\max}.
$$

Using this relation, the area of each part is obtained as follows.

$$
\text{(A)} = \alpha\, r_{\max} \times (nx), \qquad \text{(A·3)}
$$

$$
\text{(B)} = \frac{xh}{2} = \frac{1-\alpha}{2n\,(1 + \beta\,(n-1))}\, r_{\max} \times (nx), \qquad \text{(A·4)}
$$

$$
\text{(C)} = (n-1)\, xh = \frac{(1-\alpha)\,(n-1)}{n\,(1+\beta\,(n-1))}\, r_{\max} \times (nx), \qquad \text{(A·5)}
$$

$$
\begin{aligned}
\text{(D)} &= \frac{(n-1)\, x}{2}\,((1-\alpha)\, r_{\max} - h) \\
&= \frac{(1-\alpha)\,(n-1)^2\,\beta}{2n\,(1 + (n-1)\,\beta)}\, r_{\max} \times (nx). \qquad \text{(A·6)}
\end{aligned}
$$

Therefore, the throughput per flow $\langle r \rangle$ is given by

$$
\begin{aligned}
\langle r \rangle &= \frac{\text{(A)} + \text{(B)} + \text{(C)} + \text{(D)}}{nx} \\
&= \left(\alpha + \frac{1-\alpha}{2n\,(1 + \beta\,(n-1))} + \frac{(1-\alpha)\,(n-1)}{n\,(1 + \beta\,(n-1))} \right. \\
&\quad \left. + \frac{(1-\alpha)\,(n-1)^2\,\beta}{2n\,(1 + (n-1)\,\beta)} \right) r_{\max}
\end{aligned}
$$

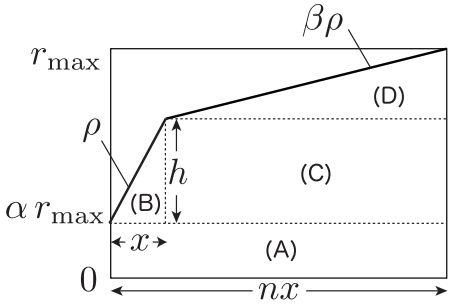

Fig. A·2 Calculation of throughput.

$$= \alpha\, r_{\max} + \frac{(1-\alpha)\,(2n-1+(n-1)^2\beta)}{2n\,(1+(n-1)\beta)}\, r_{\max}.$$

Masaki Aida received his B.S. degree in Physics and M.S. degrees in Atomic Physics from St. Paul's University, Tokyo, Japan, in 1987 and 1989, respectively, and the Ph.D. in Telecommunications Engineering from the University of Tokyo, Japan, in 1999. In April 1989, he joined NTT Laboratories. From April 2005 to March 2007, he was an Associate Professor at the Faculty of System Design, Tokyo Metropolitan University. He has been a Professor of the Graduate School of System Design, Tokyo Metropolitan University since April 2007. His current interests include traffic issues in computer communication networks. He received the Best Tutorial Paper Award of IEICE Communications Society in 2013. He is a member of the IEEE and the Operations Research Society of Japan.